IOP Conference Series:
Earth and
Environmental Science

PAPER • **OPEN ACCESS**

Edge detectors for offshore fault mapping using gravity data: Example from the Manila Trench forearc region

To cite this article: Chae Ann V. Malipol *et al* 2025 *IOP Conf. Ser.: Earth Environ. Sci.* **1517** 012017

Edge detectors for offshore fault mapping using gravity data: Example from the Manila Trench forearc region

Chae Ann V. Malipol[1], Carla B. Dimalanta[1*], Joshua Godwin Cuevas[1], Elisha Jane M. Maglalang[2] and Leo T. Armada[1]

[1] Rushurgent Working Group, National Institute of Geological Sciences, University of the Philippines, Diliman, Quezon City, Philippines
[2] Cardiff University, Cardiff, Wales, United Kingdom

*E-mail: cbdimalanta@up.edu.ph

Abstract. Multiple edge detectors (ED) are tested and applied to the gravity anomalies from the Manila Trench region. This work evaluated which ED most effectively images deformation features recently delineated in the region. Several EDs applied to the Bouguer anomalies were able to image a major strike-slip fault zone known as the West Luzon Shear Zone. The theta map of the residual Bouguer anomalies displayed sharp linear features, enabling the measurement of offsets from potential offshore splays of the Philippine Zone. Additionally, a stacked maxima heat map was created by combining ED maps, which relied on the maxima to further enhance the detection of the edge of a causative body or a linear feature.

1. Introduction

Potential fields, such as the Earth's gravitational and magnetic fields, are created by forces acting at specific points on Earth at any given time [1]. Gravity and magnetic surveys are usually conducted to measure spatial variations in these fields caused by changes in density and magnetic susceptibility at the Earth's surface. Analyzing gravity and magnetic anomalies is crucial in understanding subsurface features, including the location, geometry, and depths of the causative bodies or sources [2].

Gravity and magnetic fields are vector fields that represent forces acting at any point on the Earth's surface and are described in the x, y, and z directions [3], [4]. Filters or mathematical operators can be applied to the vector fields to enhance the fields in specific desired directions, making them suitable for delineating subsurface features or tracing linear features [5], [6], [7], [8].

Recent advancements in processing potential field data have concentrated on utilizing edge detection techniques for gravity and magnetic data. The earliest attempts to delineate the horizontal edges of these bodies led to the development of horizontal derivatives [3], [9], [10]. The techniques have progressed from simple horizontal or vertical derivatives to more sophisticated methods such as using the tilt angle or tilt derivatives, as well as mixed-class edge detectors like total horizontal gradient, horizontal derivative of the tilt derivative, theta map or tilt angle of the horizontal gradient, among others. As a result, various edge detection filters and techniques have been described in recent works.

Several authors have attempted to review the various filters proposed in numerous publications. In a study by Liu and others [11], more than 20 edge detection methods were evaluated and classified into derivative-based, phase- or ratio-based, and statistical or sliding window-based methods. Sequential methods, like the vertical derivative of the total horizontal derivative (THDR_VDR), rely on two or more derivative-based techniques. Ratio-based edge detectors, such as the theta map (TM) and normalized total horizontal derivative (TDX), are filters based on peaking normalization. Mixed class methods, such as the tilt angle of the horizontal gradient (TAHG), involve the application of both sequential and ratio class filters [11]. The study revealed differences in the resolution and reliability of the tested edge detectors and proposed using mixed-class edge detection filters for more effective results. Another review of edge detectors was carried out by [2]. They conducted a comprehensive review of more than 50 edge detection filters and proposed refinements in the mathematical applications and attributions of each edge detector.

This work examines several edge detection techniques applied to gravity data to assess their ability to reveal structural features like faults. The study evaluates and compares these filters' effectiveness in imaging faults previously mapped in the northern Manila Trench forearc region.

2. Manila Trench forearc region

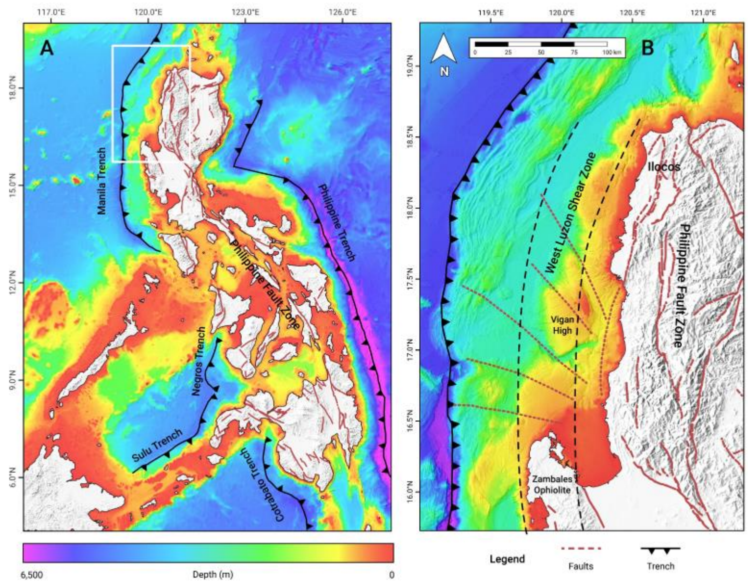

Figure 1. (a) The Philippine archipelago is bound on both sides by subduction zones. It is also bisected from northwest to southeast by the main trace of the Philippine Fault Zone (red lines). **(b)** Offshore splays of the Philippine Fault Zone (red dashed lines) were previously delineated using gravity data (modified from [12]). The trace of the West Luzon Shear Zone is modified from [13].

The convergence between the Eurasian Plate and the Philippine Sea Plate produced subduction zones on either side of the Philippine archipelago. Shear partitioning from this collision also formed the nearly 1200-km-long Philippine Fault Zone that extends from the northwestern tip of Luzon Island to the southwestern end of Mindanao Island [14]. The Manila Trench, situated west of Luzon Island, is one of the subduction zones resulting from the convergence (Figure 1a). Additionally, this convergence led to the formation of various geological features in the forearc region, including a well-formed accretionary prism, forearc basins, and volcanic arcs [15], [16], [17]. Deformation features have also been documented within the Manila Trench forearc region (Figure 1b). Karig [13] and Hayes and Lewis [16] delineated offshore faults such as the West Luzon Shear Zone, a significant left-lateral strike-slip deformation characterized by a positive free-air gravity anomaly. Moreover, they reported several northwest-trending offshore splays of the Philippine Fault. These are believed to have influenced the orientation of large submarine canyons, particularly in the northern portion of the Manila Trench forearc region (Figure 1b). A recent Armada and others [17] study reported that the Manila Trench forearc region is experiencing heterogeneous deformation along its length. They observed convergent deformation features and shearing in the southernmost parts of the forearc region, but these features were not observed in the northern forearc region. Maglalang and others [12] recently analyzed gravity data from the northern segment of the Manila Trench forearc region where the Bouguer anomaly map shows a nearly north-south arcuate belt of intermediate anomalies (~170 mGal) extending west of the Zambales Ophiolite and northward to the Ilocos region (Figure 2a). This belt is more prominent in the residual Bouguer anomaly map and is believed to coincide with the West Luzon Shear Zone previously reported by several authors (Figure 2b). This structure is interpreted as a major left-lateral strike-slip fault that translated ophiolitic blocks from the Zambales Ophiolite Complex to the Ilocos Norte region. Displacements or offsets in the residual Bouguer anomalies and tilt derivatives were used to trace several strike-slip faults within the region (Figure 1b).

3. Data and methods

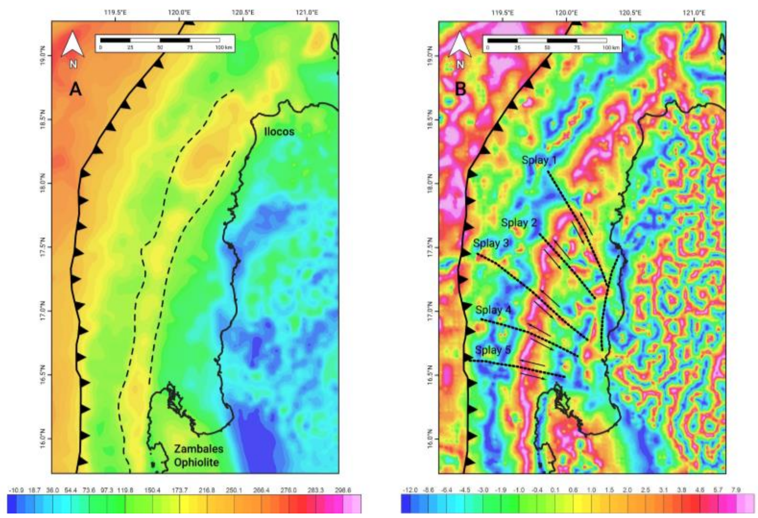

Figure 2. (a) Bouguer anomaly map for the Manila Trench forearc region. An arcuate belt of intermediate Bouguer anomalies is observed west of Luzon Island. The dashed line delineates the West Luzon Shear Zone [16]. **(b)** Tilt derivative of the Bouguer anomaly map showing the arcuate belt as a more prominent zone of high anomalies (red-pink anomalies). Offsets in the TD anomalies are used to delineate possible offshore strike-slip faults (dotted lines) (modified from [12]).

The Bouguer anomaly data for the Manila Trench region was obtained from the Bureau Gravimétrique International (BGI) (https://bgi.obs-mip.fr/grids-and-models-2/). The BGI calculated the Bouguer anomalies from the Earth Gravitational Model (EGM2008) using the FA2BOUG code developed by [18]. The Bouguer anomalies were gridded and visualized using the Oasis Montaj software (Figure 2a). The radially averaged power spectrum (RAPS) of the Bouguer anomaly was calculated to determine the depths where deep (regional) and shallow (residual) bodies occur. An upward continuation filter was then applied to obtain the regional Bouguer anomaly. The regional Bouguer anomaly was subtracted from the Bouguer anomaly to remove the effects of deep sources and retain the signals of shallow features. The resulting anomalies were used to generate the residual Bouguer anomaly map, which depicts bodies at depths of 2.5 km (Figure 2b).

For this work, both the Bouguer and residual Bouguer anomalies were subjected to enhancements. These include standard edge detection techniques such as directional derivatives (X, Y, and Z), tilt derivatives, analytic signals (AS), and horizontal gradients. Table 1 summarizes

Table 1. Equations for the standard edge detection methods and their interpretation.

Edge detection method	Equation	Interpretation of anomaly
1st order horizontal derivative (FHD) [19]	$FHD = \sqrt{\left(\frac{\partial G}{\partial x}\right)^2 + \left(\frac{\partial G}{\partial y}\right)^2}$ where $\frac{\partial G}{\partial x}$ and $\frac{\partial G}{\partial y}$ are the horizontal derivatives of the gravity field (G) in the x and y directions.	maxima = source edge or linear feature
1st vertical derivative (VDR) [20]	$VDR = \frac{\partial G}{\partial z}$	zero = source edge or linear feature
Total horizontal derivative (THDR) [21]	$THDR = \sqrt{\left(\frac{\partial G}{\partial x}\right)^2 + \left(\frac{\partial G}{\partial y}\right)^2}$	maxima = source edge or linear feature
Tilt derivative (TDR) [22]	$TD = \tan^{-1}\left(\frac{VDR}{THDR}\right)$	zero = source edge or linear feature
Total Horizontal Derivative of the Tilt Derivative (TDR THDR) [23]	$TDR\ THDR = \sqrt{\left(\frac{\partial TD}{\partial x}\right)^2 + \left(\frac{\partial TD}{\partial y}\right)^2}$	maxima = source edge or linear feature

the directional derivative filters applied to gravity data and the interpretation of the resulting anomalies, i.e., whether the maxima or zero anomalies define a linear feature or the edge of the source or causative body.

Edge detectors such as the VDR and TDR have performed well in imaging shallow sources with substantial density contrasts [24], [25]. Generally, mixed-class filters have performed better than the other two classes. The TAHG filter was found to produce fewer false edges [26]. Ratio and normalization classes were also advantageous since the signals between the deep and shallow sources were more balanced.

Several combination filters were also tested in this work, such as the total horizontal derivative of the tilt derivative, normalized total horizontal derivative (TDX), vertical derivative of the total horizontal derivative (THDR_VDR), theta map (TM), and tilt angle of the horizontal gradient (TAHG) filters (Table 2).

Table 2. Combination of edge detection methods tested and their classification.

Edge detection method	Equation	Classification
Vertical derivative of the total horizontal derivative (THDR_VDR) [27]	$THDR\ VDR = \frac{\partial THDR}{\partial z}$	Sequential combination
Theta Map (TM) [28]	$\cos \Theta = \frac{THDR}{AS}$	Ratio-based
Normalized Total Horizontal Derivative (TDX) [24]	$TDX = \tan^{-1}\left(\frac{THDR}{\lvert VDR \rvert}\right)$	Ratio-based
Tilt angle of the horizontal gradient (TAHG) [26]	$TAHG = \tan^{-1}\left(\frac{\frac{\partial THDR}{\partial z}}{\sqrt{\left(\frac{\partial THDR}{\partial x}\right)^2 + \left(\frac{\partial THDR}{\partial y}\right)^2}}\right)$	Mixed class

Moreover, after applying the enhancements, we proposed generating a stacked maxima heat map. A heat map is usually generated to visualize point density or the areas with the most point features [29]. This is commonly used in Geographic Information System (GIS) where several raster maps are stacked on top of each other to produce susceptibility maps. Following this principle, we applied this technique to edge detectors to reduce random signals, enhance features consistent across individual filters, and produce clearer images. The edge detectors yield a corresponding value depending on the gradient of the gravity anomaly at a particular location (e.g., mGal/m for THDR). The enhanced maps were combined or stacked together to highlight the maxima or large gravity changes which may indicate the edge of a causative body or a linear feature. In stacking the enhanced maps, the output Geosoft grid files were converted to a Surfer 7 grid file to produce a single-color band using the grid features of Oasis Montaj. The converted grid files were loaded into the QGIS software. Using the raster calculator function, all the enhanced maps using maxima were added together to create the stacked maxima heat map.

4. Results and discussion

In a previous study of gravity data from the Manila Trench forearc region, Maglalang and others [12] identified a prominent arcuate belt of gravity anomalies west of Luzon Island (Figures 2a and 2b). This was interpreted to define the West Luzon Shear Zone, a major strike-slip fault associated with translating blocks from the Zambales Ophiolite northward to the Ilocos region [12]. In addition, five strike-slip faults were delineated based on the observed displacements in the belt of high gravity anomalies (Figure 2b). These displacements suggest the presence of left-lateral strike-slip faults, which are interpreted to be potential offshore extensions of the

Philippine Fault Zone. This study employed different edge detection methods to identify the best filter for accurately visualizing the offsets or displacements in the delineated faults. These edge detection methods were applied to both Bouguer anomalies and residual Bouguer anomalies, and we discuss the differences in the derivative maps generated from these methods.

Figures 3a to 3j present the different maps of the Bouguer anomaly enhanced using various filters. The belt of high Bouguer anomalies west of Luzon Island is observed in the directional derivative maps, such as the first-order horizontal X (FHDx), first-order vertical derivative (1VDR) and tilt derivative maps (Figures 3a, 3c and 3e). Combinations of enhancement methods were also applied. The arcuate belt is clearly shown in the TDX, theta map, TAHG, and THDR_VDR (Figures 3g-3j). However, due to its primarily north-south trend, the first-order horizontal Y derivative map cannot cohesively resolve the belt (Figure 3b). The THDR filter, which combines the X and Y horizontal derivatives, shows differences in the amplitude of the maxima that defines the arcuate belt west of Luzon Island. The arcuate belt is less distinctly imaged in the THDR map, as zones of maxima are also seen east of the arcuate belt closer to the western part of Luzon Island (Figure 3d). The TDR THDR was proposed by Fairhead and others [23] to enhance magnetic data since it is not affected by the inclination of the magnetic field. This filter was applied to the gravity data from the Manila Trench region to see how the filter performs. However, the resulting TDR THDR did not yield a clear or cohesive image of the arcuate belt (Figure 3f).

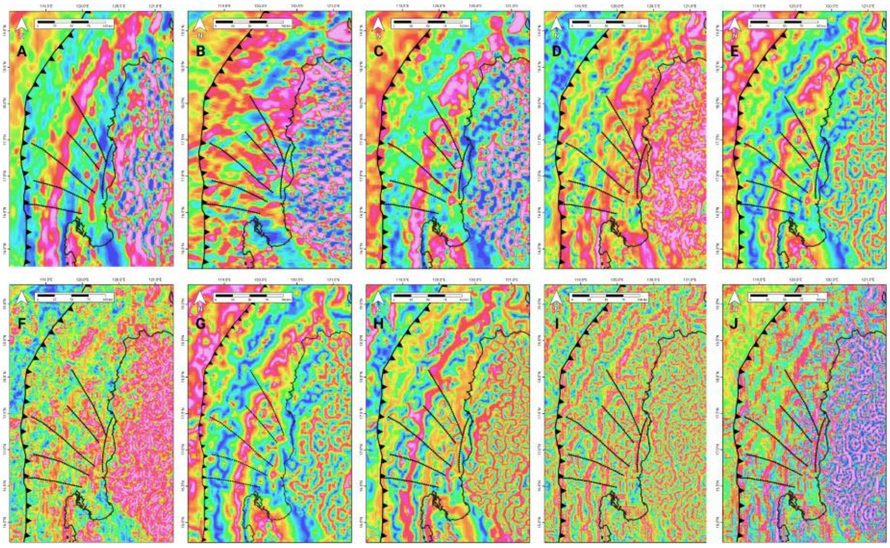

Figure 3. Edge detection enhancements applied to Bouguer anomalies - **(a)** first order horizontal x derivative (FHDx), **(b)** first order horizontal y derivative (FHDy), **(c)** first order vertical derivative (1VDR), **(d)** total horizontal derivative (THDR), **(e)** tilt derivative (TD), **(f)** total horizontal derivative of the tilt derivative (TDR THDR), **(g)** normalized total horizontal derivative (TDX), **(h)** theta map (TM), **(i)** tilt angle of the horizontal gradient (TAHG) and **(j)** vertical derivative of the THDR (THDR_VDR).

The same enhancements or edge detectors were applied to the residual Bouguer anomalies. The arcuate belt west of Luzon can be more clearly traced in the FHDx, 1VDR, THDR, TD, TDX, and TM (Figures 4a, 4c, 4d, 4e, 4g, and 4h). It can be observed that the arcuate belt is narrower than the belt imaged in the enhanced Bouguer anomaly maps, suggesting a more precise delineation of the structural feature. Although the arcuate belt is still visible in the TAHG and THDR_VDR maps (Figures 4i and 4j), the derivatives are not as sharp as those observed in the same enhancements applied to the Bouguer anomalies (Figures 3i and 3j). Some authors have reported the low resolution of source edges to be a limitation of the TAHG [30]. The diffuse anomalies observed in the TDR_THDR show that this filter is also not as effective in outlining the edges of the arcuate belt delineated in the other maps (Figure 4f).

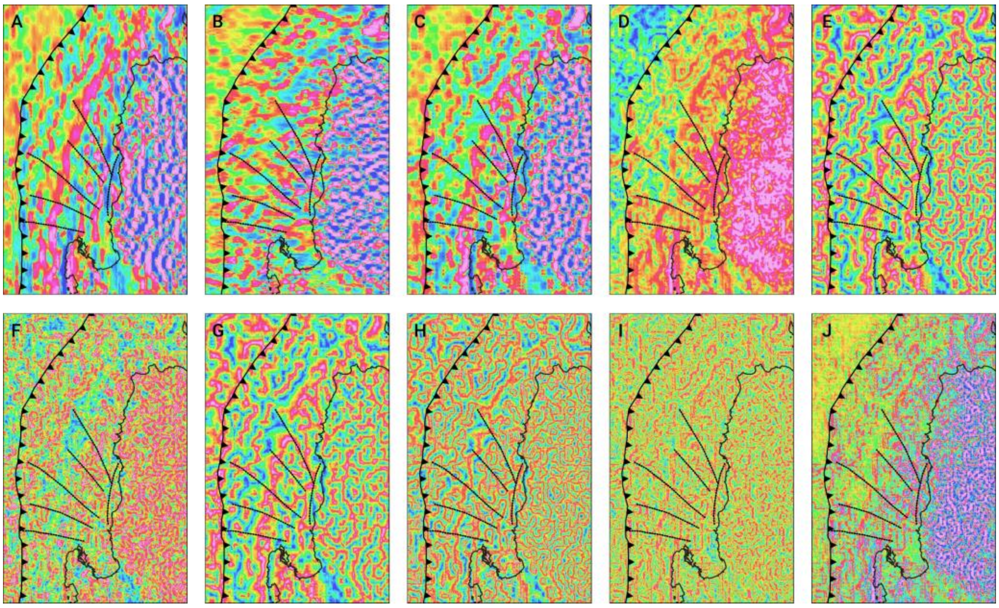

Figure 4. Edge detection enhancements applied to residual Bouguer anomalies - - **(a)** first order horizontal x derivative (FHDx), **(b)** first order horizontal y derivative (FHDy**), (c)** first order vertical derivative (1VDR), **(d)** total horizontal derivative (THDR), **(e)** tilt derivative (TD), **(f)** total horizontal derivative of the tilt derivative (TDR THDR), **(g)** normalized total horizontal derivative (TDX), **(h)** theta map (TM), **(i)** tilt angle of the horizontal gradient (TAHG) and **(j)** vertical derivative of the THDR (THDR_VDR).

The edge detectors were also evaluated to determine whether these will allow the measurement of the offsets or displacements in the possible offshore splays of the Philippine Fault Zone previously reported by Maglalang and others [12] (Figure 2b). These discontinuities in the arcuate belt of gravity anomalies caused by the offshore splays are best observed in the enhancements of the Bouguer anomalies, such as the THDR, TD, TDX, TAHG, and THDR_VDR of the Bouguer anomalies (Figures 3d, 3e, 3g, 3i and 3j). The maxima in the enhanced maps show step-like signatures suggesting offsets or displacements from their original position.

Furthermore, the offsets are more visible in the enhanced residual Bouguer anomaly maps such as TD, TDX, theta map, TAHG, and THDR_VDR. The offsets in the proposed offshore splays can be best estimated in the theta map (Figure 4h).

In the stacked maxima heat map of the enhanced Bouguer anomalies (Figures 5a and 5b), the step-like signatures indicating displacements are prominently displayed in red. This suggests that these areas appear as maxima in the different enhanced maps. The displacements vary from around 12 kilometers for Splay 3 to approximately 8 kilometers for Splay 4 (Figure 5b).

The generated stacked maxima heat map precisely defines the trace of the West Luzon Shear Zone. This coincides with the edge of the bathymetry high, suggesting that the West Luzon Shear Zone is a linear and narrow feature, different from the delineated zone in Figure 2. Additionally, our results can be validated since the anomalies from the stacked map can delineate the nearly north-south onshore trace of the Philippine Fault Zone in the Ilocos region (Figure 1b).

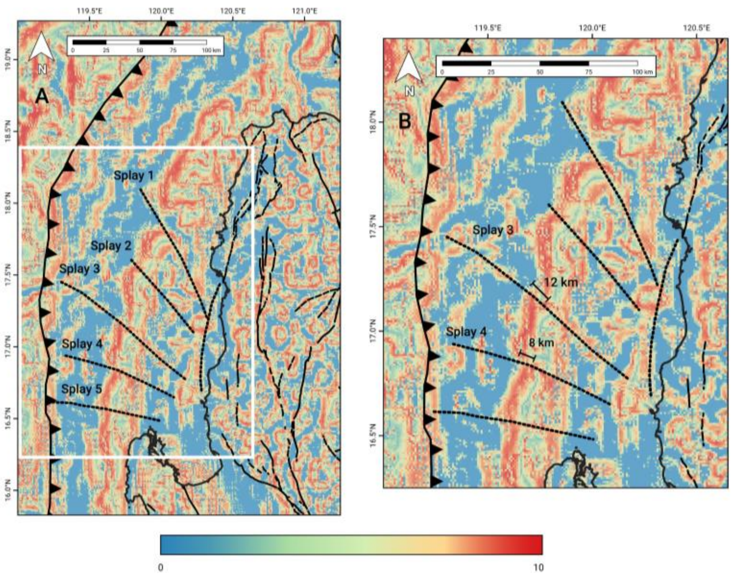

Figure 5. (left) Stacked maxima heat map of the Bouguer anomalies. (right) Zoomed in view of the displacements in the maxima, which are used to delineate the possible offshore splays of the Philippine Fault (dotted lines). The horizontal displacements are measured from each end of the displaced segment of the maxima. Lateral offsets are shown for Splay 3 (12 km) and Splay 4 (8 km).

5. Conclusions

Several available edge detectors were applied to gravity data from the Manila Trench forearc region. Among the enhancements applied to the Bouguer anomalies, the FHDx, 1VDR, TD, TDX, TM, TAHG, and THDR_VDR maps imaged the arcuate belt west of Luzon Island. However, the arcuate belt was narrower and sharper in the TD and TDX maps. The TD, TDX, and TM filters of the residual Bouguer anomalies produced sharp edges that delimit the arcuate belt. In addition, stacking the enhancement results further refined the identified boundary by providing a more precise image. This method enhances signals consistent across individual filters while minimizing random features, resulting in sharper linear features. The TM of the residual Bouguer anomalies allowed estimates of the displacements observed in the offshore splays of the Philippine Fault Zone. Offsets are estimated to range from ~5 to 30 kilometers from the southern splay to the northern splay.

Acknowledgment

The authors acknowledge the research grant provided by the Philippine Department of Science and Technology for the project "Marine and onshore geophysical investigations of the Manila subduction zone. A NIGS research grant to CBD is also gratefully acknowledged. Discussions with members of the Rushurgent Working Group are also gratefully acknowledged.

References

[1] Mickus K 1980 Gravity method *Geophysics* **45** 83–87

[2] Nuñez-Demarco P, Bonilla A, Sanchez Bettucci L and Prezzi C 2023 Potential-field filters for gravity and magnetic interpretation: A review *Surveys in Geophysics* **44** 603–664

[3] Saad A H 2006 Understanding gravity gradients - a tutorial *The Leading Edge* **25** 942–949

[4] Al-Banna A S 2021 Gravity Field Theory *Gravitational Field - Concepts and Applications* ed Essa K S (IntechOpen)

[5] Ma G and Li L 2012 Edge detection in potential fields with the normalized total horizontal derivative *Computers & Geosciences* **41** 83–87

[6] Nguimbous-Kouoh J J, Ngos III S and Manguelle-Dicoum 2019 Using EGM2008 Gravity Data for Mapping and Detecting Structural Subsurface Anomalies in the Mayo-Kani Division (Cameroon) *Journal of Geosciences and Geomatics* **7** 42–53

[7] Eldosouky A M, Pham L T and Henaish A 2022 High precision structural mapping using edge filters of potential field and remote sensing data: A case study from Wadi Umm Ghalqa area, South Eastern Desert, Egypt *The Egyptian Journal of Remote Sensing and Space Sciences* **25** 501–513

[8] Pham L T, Van Duong H, Kieu Duy T, Oliveira S P, Lai G M, Bui T M and Oksum E 2023 An effective edge detection technique for subsurface structural mapping from potential field data *Acta Geophysica* **72** 1661–1674

[9] Rosid M S and Siregar H 2017 Determining fault structure using first horizontal derivative (FHD) and horizontal vertical diagonal maxima (HVDM) method: A comparative study *2nd International Symposium on Current Progress in Mathematics and Sciences*

[10] Cheunteu Fantah C A, Mezoue C A, Mouzong M P, Tokam Kamga A P, Nouayou R and Nguiya S 2022 Mapping of major tectonic lineaments across Cameroon using potential field data *Earth, Planets and Space* **74** Article 59

[11] Liu J, Wang X, Suo Y, Li S and Zhou J 2023 A robust high-resolution potential-field edge detection filter with its application in the Indo-China Peninsula *Tectonophysics* **868** 230109

[12] Maglalang EJM, Armada LT, Dimalanta CB, Sayen KF, Eleazar BD, Parcutela NE, Austria RS, Yumul GP Jr and Hsu S-K 2024 *Journal of Asian Earth Sciences*. Submitted

[13] Karig D 1983 Accreted terranes in the northern part of the Philippine archipelago *Tectonics* **2** 211–236

[14] Fitch TJ Plate convergence, transcurrent faults, and internal deformation adjacent to Southeast Asia and the Western Pacific 1972 *Journal of Geophysical Research* **77** 4432–4460

[15] Ludwig W J, Hayes D E and Ewing J I 1967 The Manila Trench and West Luzon Trough–I. Bathymetry and sediment distribution *Deep Sea Research and Oceanographic Abstracts* **14** 533–544

[16] Hayes D E and Lewis S D 1985 Structure and tectonics of the Manila trench system, Western Luzon, Philippines *Energy* **10** 263–279

[17] Armada L T, Hsu S-K, Dimalanta C B, Yumul G P Jr, Doo W-B and Yeh Y-C 2020 Forearc structures and deformation along the Manila Trench *Journal of Asian Earth Sciences: X* **4** 100036

[18] Fullea J, Fernandez M and Zeyen H 2008 FA2BOUG – A FORTRAN 90 code to compute Bouguer gravity anomalies from gridded free-air anomalies: Application to the Atlantic-Mediterranean transition zone *Computers & Geosciences* **34** 1665–1681

[19] Cordell L and Grauch V J S 1985 Mapping basement magnetization zones from aeromagnetic data in the San Juan Basin, New Mexico *The utility of regional gravity and magnetic anomaly maps* ed W J Hinze (Society of Exploration Geophysicists, Tulsa) pp 181–197

[20] Ackerman H A and Dix C H 1955 The first vertical derivative of gravity *Geophysics* **20** 148–154

[21] Cordell L 1979 Gravimetric expression of graben faulting in Santa Fe country and the Espanola Basin, New Mexico *Guidebook to Santa Fe Country* ed RV Ingersoll, LA Woodward and HL James (New Mexico Geological Society) pp 59–64

[22] Miller H G Singh V 1994 Potential field tilt—a new concept for location of potential field sources *Journal of Applied Geophysics* **32** 213–217

[23] Fairhead J D, Mackenzie C, Green C M and Verduzco B 2004 A new set of magnetic field derivatives for mapping mineral prospects *ASEG Extended Abstracts* **1** 1–4

[24] Cooper G and Cowan D R 2006 Enhancing potential field data using filters based on the local phase *Computers & Geosciences* **32** 1585–1591

[25] Ekinci Y L, Ertekin C and Yiğitbaş E 2013 On the effectiveness of directional derivative based filters on gravity anomalies for source edge approximation: synthetic simulations and a case study from the Aegean graben system (western Anatolia, Turkey) *Journal of Geophysics and Engineering* **10** 035005

[26] Ferreira F J, de Souza J, de Bongiolo B E S A and de Castro L G 2013 Enhancement of the total horizontal gradient of magnetic anomalies using the tilt angle *Geophysics* **78** J33–J41
[27] Hood P J and Teskey D J 1989 Aeromagnetic gradiometer program of the Geological Survey of Canada *Geophysics* **54** 1012–1022
[28] Wijns C, Perez C and Kowalczyk P 2005 Theta map: Edge detection in magnetic data *Geophysics* **70** L39–L43
[29] Wilkinson L and Friendly M 2012 The history of the cluster heat map *The American Statistician* **63** 179-184
[30] Prasad K N D, Pham L T, Singh A P, Eldosouky A M, Abdelrahman K, Fnais M S and Gómez-Ortiz D 2022 A novel Enhanced Total Gradient (ETG) for interpretation of magnetic data *Minerals* **12** 1468